Energy Conversion and Management 327 (2025) 119545

Contents lists available at ScienceDirect

Energy Conversion and Management

journal homepage: www.elsevier.com/locate/enconman

Thermodynamic, thermoeconomic, and exergoeconomic analysis of a UAV two stroke engine fueled with gasoline-octanol and gasoline-hexanol blends

Salih Özer [a], Erdal Tunçer [b,c], Usame Demir [d], Halil Erdi Gülcan [e,*]

[a] Department of Mechanical Engineering Muş Alparslan University Muş Turkiye
[b] Erin Engine Corporation Inc. Department of Research and Development Istanbul Turkiye
[c] Department of Mechanical Engineering Faculty of Engineering and Natural Sciences Istanbul Health and Technology University Istanbul Turkiye
[d] Department of Mechanical Engineering Bilecik şeyh Edebali University Bilecik Turkiye
[e] Department of Mechanical Engineering Faculty of Technology Selcuk University Konya Turkiye

ARTICLE INFO

Keywords:
Energy and exergy analysis
Exergoeconomic
Hexanol
Octanol
Thermoeconomic
Two stroke engine

ABSTRACT

In recent years, as the use of Unmanned Aerial Vehicle (UAV) engines has increased in various application areas such as military fields, defense, emergencies, and mapping, the use of these engines with fossil-based fuels has raised environmental concerns. The addition of heavy alcohols such as octanol and hexanol, which have high energy densities, to the fossil-based fuels used may help reduce environmental concerns and contribute to performance improvement. In this study, the performance, emissions, thermodynamic, thermoeconomic, and exergoeconomic analysis of a two-stroke engine operating with gasoline-octanol and gasoline-hexanol fuels in a UAV is conducted. There are no studies in the literature that examine the energy, exergy, thermoeconomic, and exergoeconomic aspects of a two-stroke UAV engine operating with gasoline-octanol and gasoline-hexanol fuel mixtures. The aim of this study is to understand the performance and emission characteristics of used heavy alcohols such as octanol and hexanol in a two-stroke UAV engine, and to examine them from a thermodynamic perspective. The experiments are carried out at different shaft speed ranges (3250, 3750, 4500, 5250, and 6250 rpm). Additionally, seven different fuels are used in the experiments: gasoline, gasoline-octanol mixtures (volumetrically 10 %, 20 %, and 30 %), and gasoline-hexanol mixtures (volumetrically 10 %, 20 %, and 30 %). The results show that increasing the octanol content in gasoline to 30 % (OC30) reduces the specific fuel consumption (SFC) by up to 5.5 % (at 6250 shaft speed), while increasing the hexanol content to 30 % (HX30) increases it by 6 % (at 5250 shaft speed). CO emissions decrease by an average of 5.3 % and 9.2 % with OC30 and HX30 fuels, respectively (both at 6250 shaft speed), while CO_2 emissions increase by an average of 3 % and 10 % with OC30 and HX30 fuels, respectively. With OC30 fuel, the exergetic destruction decreases by an average of 6 % compared to gasoline, while with HX30 fuel, it increases by an average of 3.3 %. OC30 increases the exergetic efficiency by an average of 5.4 % compared to gasoline, whereas HX30 decreases it by 2.9 %.

1. Introduction

Internal combustion engines (ICEs) have been integral to transportation, power generation, and machinery for over a century, powering everything from cars and trucks to generators and marine vessels [1,2]. However, ICEs are also major sources of air pollution, emitting a variety of pollutants including carbon monoxide (CO), hydrocarbons (HC), nitrogen oxides (NO_x), and particulate matter (PM)[3,4]. The environmental and health impacts of these emissions have spurred stringent regulations and the development of advanced emission control technologies[5,6]. As a result, emissions control in internal combustion engines has become a significant area of research, focusing on improving combustion efficiency and reducing harmful emissions[7,8]. The integration of hydrogen and water injection strategies in rotary and dual-fuel engines can significantly enhance combustion efficiency and reduce emissions[9]. The design of combustion chambers and the optimization of injection rate shapes are critical factors in achieving these improvements[10–12]. By carefully selecting and implementing these strategies, it is possible to enhance engine performance while minimizing environmental impact. Various methods are employed to control emissions in internal combustion engines, including after-treatment systems like catalytic converters and particulate filters, as well as in-

* Corresponding author.
E-mail addresses: halilerdigulcan@gmail.com, halil.gulcan@selcuk.edu.tr (H.E. Gülcan).

https://doi.org/10.1016/j.enconman.2025.119545
Received 16 November 2024; Received in revised form 30 December 2024; Accepted 18 January 2025
Available online 29 January 2025

cylinder technologies such as exhaust gas recirculation (EGR) [13], lean-burn strategies[7], and advanced fuel injection systems[14]. Catalytic converters, for instance, help convert CO, HC, and NO_x into less harmful gases like CO_2, H_2O, and N_2. EGR recirculates a portion of exhaust gases back into the intake air, lowering peak combustion temperatures to reduce NO_x formation[15,16]. While these technologies have significantly reduced emissions in traditional ICE applications, they are often complex and add weight, making them less suitable for compact, lightweight engines used in unmanned aerial vehicles (UAVs)[17].

UAVs, commonly known as drones, have seen a dramatic rise in usage across various industries, including agriculture, surveillance, logistics, and environmental monitoring[18,19]. Unlike conventional aircraft, UAVs typically operate on small, lightweight engines, often two-stroke ICEs due to their high power-to-weight fraction, simplicity, and reliability[20]. Two-stroke engines provide high performance with fewer moving parts compared to four-stroke engines, making them ideal for the weight and space constraints in UAVs[21]. However, two-stroke engines have inherent design limitations that result in higher emissions. During the scavenging process in two-stroke engines, fresh air–fuel mixtures can escape with the exhaust gases, leading to incomplete combustion and higher levels of HC and CO emissions. This inefficiency in the combustion process, combined with the high usage of UAVs, underscores the importance of exploring cleaner fuels and fuel blends to mitigate the environmental impact of UAV operations[22].

In recent years, researchers have turned to alternative fuels as potential solutions to reduce emissions and improve the efficiency of ICEs, including those in UAVs. Among these alternative fuels, alcohol-based fuels have garnered significant interest due to their cleaner combustion characteristics and potential for renewable production[23]. Alcohols such as ethanol and methanol have long been used as gasoline additives or replacements in automotive engines. They burn more cleanly than gasoline, producing lower amounts of CO, HC, and particulate emissions. Furthermore, alcohols are oxygenated fuels, meaning they contain oxygen within their molecular structure. This oxygen content promotes more complete combustion, which can reduce the production of pollutants associated with incomplete combustion, such as CO and HC. The use of higher alcohols, such as octanol and hexanol, as alternative fuels has garnered significant attention due to their potential to enhance engine performance and reduce emissions. Despite the growing interest, studies specifically focusing on their effects on two-stroke engines remain limited. Prior research has extensively explored the impact of alternative fuels on combustion characteristics, emissions, and efficiency. For instance, investigations into the broader application of oxygenated fuels have highlighted their potential in reducing particulate emissions and improving combustion stability [24]. Further, studies on high-pressure direct injection systems have demonstrated the critical role of fuel properties in optimizing engine performance and emissions [25]. Moreover, comparative analyses of oxygenated diesel fuels have provided insights into the spray characteristics and combustion dynamics, underscoring the importance of fuel formulation [26]. Building on these foundations, the present study aims to investigate the specific effects of higher alcohols, such as octanol and hexanol, on the performance and emissions of two-stroke engines, addressing a critical gap in the existing body of knowledge. While ethanol and methanol have been widely studied and used in commercial automotive applications, their relatively low energy density and high volatility pose challenges, particularly in high-performance and UAV engines [27]. Ethanol and methanol are low-carbon alcohols with high vapor pressures, meaning they are prone to evaporation losses and may require special handling and storage procedures. Moreover, their lower energy content compared to gasoline means that they provide less energy per liter, which can lead to a reduction in fuel economy and power output if not used in optimized engine configurations. To overcome these limitations, researchers have been exploring the use of higher alcohols, specifically octanol and hexanol, as potential biofuel alternatives for internal combustion engines[28]. Higher alcohols, such as octanol ($C_8H_{18}O$) and hexanol ($C_6H_{14}O$), offer several advantages over lower alcohols like ethanol and methanol. Due to their longer carbon chains, octanol and hexanol have higher energy densities, closer to that of gasoline, which allows them to deliver more energy per unit volume. This higher energy content makes them more suitable for applications where high power output and energy efficiency are essential, such as UAV engines[29]. Additionally, octanol and hexanol have lower vapor pressures and higher flash points compared to ethanol and methanol, reducing the risk of evaporation losses and making them safer to handle and store under typical operating conditions. Octanol and hexanol possess several fuel characteristics that make them promising candidates for improving combustion quality and emissions control in internal combustion engines[30,31]. Octanol has a research octane number (RON) of approximately 106, which is higher than that of gasoline, providing superior resistance to knocking. This property is particularly advantageous for high-compression engines, as it allows for more stable combustion without the risk of pre-ignition or knock. Knock resistance is essential in engines designed for high performance, as knocking can cause mechanical damage and reduce engine efficiency[32]. Hexanol, although having a lower RON (around 73), still offers benefits due to its oxygen content, which promotes more complete combustion and reduces CO and HC emissions[33]. The oxygen content in octanol and hexanol is one of the primary reasons they are attractive as biofuel blends. Oxygenated fuels enable more efficient oxidation of carbon and hydrogen atoms during combustion, resulting in cleaner exhaust gases[34]. The presence of oxygen in the fuel structure helps reduce emissions of pollutants like CO and HC, which are typically associated with incomplete combustion [35]. However, oxygenated fuels can lead to increased CO_2 emissions, as the additional oxygen allows for more complete combustion, converting more of the carbon content in the fuel to CO_2 [36]. Therefore, while octanol and hexanol can help reduce harmful pollutants, managing CO_2 emissions remains a crucial aspect of optimizing their use as biofuels [37,38]. Despite their promising characteristics, research on octanol and hexanol as fuel blends in UAV engines is still limited. Most studies on higher alcohols have focused on automotive applications[39], with little exploration of their effects on small, lightweight engines. UAV engines, particularly two-stroke engines, have unique operational requirements and challenges that differ from automotive engines. The simplicity of two-stroke engines, while beneficial for reducing weight and complexity, leads to higher emissions due to the overlap between exhaust and intake cycles. This overlap allows some of the fresh air–fuel mixture to escape with the exhaust gases, leading to incomplete combustion. Given these characteristics, two-stroke UAV engines stand to benefit significantly from the cleaner combustion properties of oxygenated fuels like octanol and hexanol.

In this study, we investigate the effects of gasoline-octanol and gasoline-hexanol blends on a two-stroke, UAV engine, focusing on performance, emissions, energy, exergy, thermoeconomic, and exergoeconomic. By blending gasoline with varying proportions of octanol and hexanol, we aim to determine whether these higher alcohols can improve combustion quality, reduce SFC, and lower emissions. Furthermore, this study will examine the exergy efficiency of each fuel blend, providing insights into how effectively each fuel converts energy into useful work and where energy losses occur. The results are expected to contribute to the development of cleaner, more efficient UAV engines and demonstrate the potential of higher alcohols as viable biofuel alternatives for internal combustion engines in aviation applications.

2. Test setup and methodology

2.1. Test setup

The experiments were conducted using a custom-designed engine test cabinet specifically tailored for a two-stroke internal combustion engine intended for an Unmanned Aerial Vehicle (UAV). The technical specifications of the engine are given in Table 1.

Table 1
The technical specifications of the two stroke UAV engine.

Technical Details	Unit	Value
Brand and Model	–	Erin Motor and Baykuş
Number of cylinders	–	Two
Cooling system	–	Air Cooled
Diameter	mm	48
Stroke	mm	36.5
Total cylinder volume	L	0.132
Peak power (at 8000 1/min)	Hp	12
Compression ratio	–	10.4:1
Idle speed	rpm	1800

Also, the test setup shown schematically in Fig. 1 includes various components such as a fuel metering device, adjustable power unit, thermal camera, load cell, exhaust gas outlet, and an emission measurement device. The engine was tested at various shaft speeds (3250, 3750, 4500, 5250, and 6250 rpm) to simulate a range of operating conditions and obtain a comprehensive data set. These speeds were chosen within the engine's operational range, where the idling speed is 1800 rpm, and maximum power is achieved at 8000 rpm. This selection ensures coverage of both low-load and high-load conditions while avoiding extremes that might compromise data reliability.

Controls and measures the exact fuel flow rate to the engine, ensuring consistency across tests. Regulates power to the engine system, allowing for controlled engine speed and load adjustments. It was positioned to monitor and record engine casing temperature in real time. It has a range from −10 °C to 1000 °C (with a precision of ± 2°C), enabling precise temperature measurements under various operational states. Load cell attached to the propeller, this device measures thrust generated by the engine with a precision of ± 0.01 kg, which is critical for assessing engine performance. BOSCH BEA 060 gas analyzer is connected to the exhaust gas outlet to measure the concentrations of CO, CO_2, HC, O_2, and NO_x emissions. This analyzer provides real-time emissions data, essential for evaluating the environmental impact of each fuel blend. The entire setup was calibrated before each test run to ensure data accuracy and repeatability. The calibration involved verifying the readings from each sensor and adjusting the measurement devices as needed based on standard procedures.

2.2. Fuel mixtures and blending ratios

Seven fuel blends were tested in this study, each with a specific gasoline and bio-alcohol composition. Gasoline was blended with either octanol or hexanol in volumetric proportions of 10 %, 20 %, and 30 %. The fuel mixtures and corresponding abbreviations are presented in Table 2.

Each blend was prepared immediately prior to testing to prevent potential phase separation or chemical degradation. The hexanol (Purity: 98 %, CAS No: 108–93-0) and octanol (Purity: 99 %, CAS No: 111–87-5) were obtained from Merck Millipore to ensure reliable and consistent quality for the experiments. The octanol and hexanol were obtained in pure form and mixed thoroughly with gasoline to ensure homogeneity. These bio-alcohols were chosen due to their high energy

Table 2
Blending ratio and fuel mixture abbreviations.

Fuel No	Blending ratio	Abbreviations
1	Gasoline – 100 % vol.	G100
2	Gasoline – 90 %vol. + Octanol – 10 %vol	OC10
3	Gasoline – 80 %vol. + Octanol – 20 %vol	OC20
4	Gasoline – 70 %vol. + Octanol – 30 %vol	OC30
5	Gasoline – 90 %vol. + Hexanol – 10 %vol	HX10
6	Gasoline – 80 %vol. + Hexanol – 20 %vol	HX20
7	Gasoline – 70 %vol. + Hexanol – 30 %vol	HX30

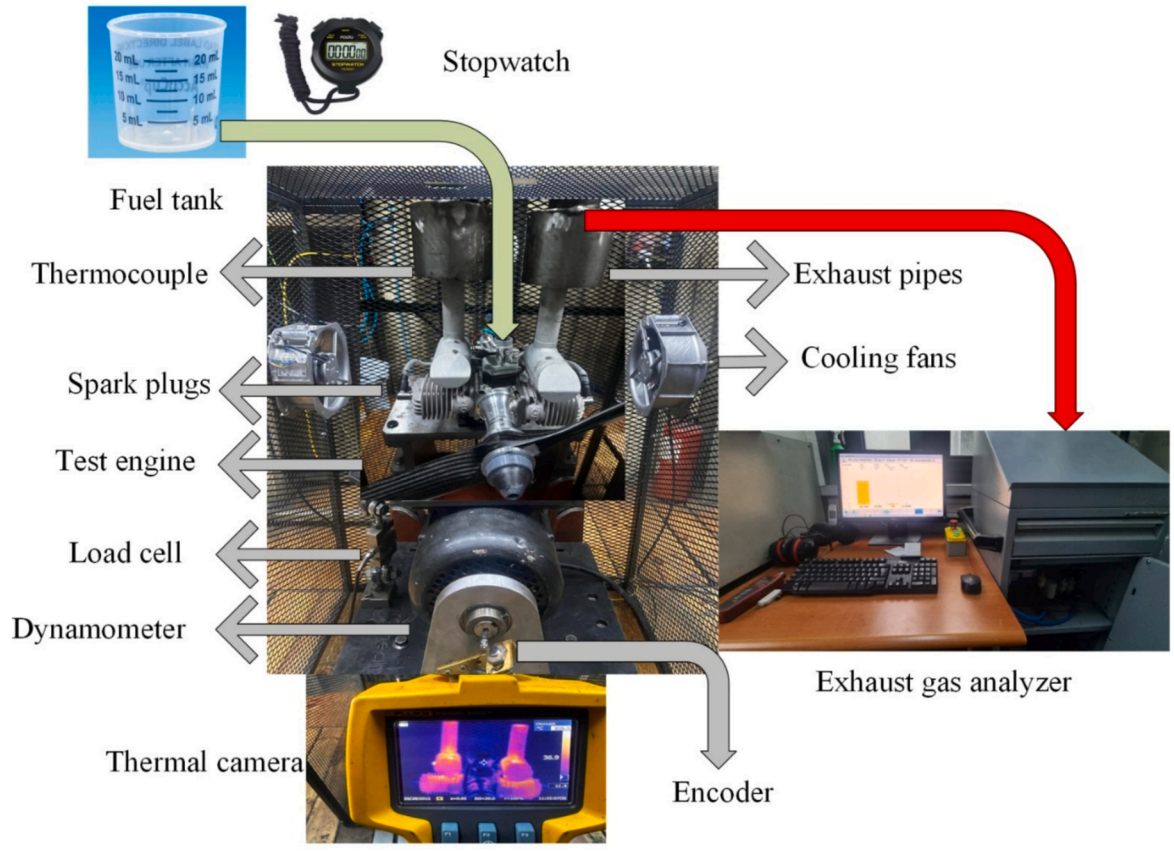

Fig. 1. Experimental Test Schematic Diagram.

content and potential to reduce emissions when blended with gasoline. The properties of octanol, hexanol and gasoline fuels are presented in Table 3.

2.3. Measurement devices and parameters

High-precision instruments were employed to record various operational parameters, such as shaft speed, thrust force, performance parameters, surcafe temperature, and exhaust emissions. A laser tachograph meter ranging from 2.5 to 99,999 rpm and a 1 rpm resolution was used to continuously monitor engine speed. The meter had an additional uncertainty of 0.5 % due to inherent variability across repeated measurements. The thrust generated by the engine's propeller was recorded using an 'S' type load cell, providing precise measurements at a resolution of ± 0.01 kg and accounting for a calibration-related uncertainty of ± 0.1 %. Fuel flow meter was recorded by timing the duration required to burn a fixed 20 ml volume of fuel using a chronometer (accuracy ± 0.1 s). Fuel amount was also recorded with a precision of ± 0.1 ml, and these uncertainties were included in the calculation of SFC. The Surface fin temperature was recorded with a thermal cam device capable of measuring up to 1000 °C (with a ± 2°C uncertainty). Exhaust gas temperatures were measured by a K-type thermocouple (with an accurancy of ± 0.1 °C) to monitor the thermal behavior of the engine under different fuel conditions. BOSCH BEA60 emission device measured CO, CO_2, HC, O_2, and NO_x emissions. This device allowed for high-precision recording of emission levels, critical for assessing the environmental impact of each fuel blend. The analyzer was calibrated before each test to ensure accuracy. Table 4 summarizes the key parameters measured during the experiments, the sensitivity of the devices used, the associated tolerances, and relevant remarks about the uncertainties involved. This ensures transparency regarding the accuracy and reliability of the experimental data.

The data obtained from the experiments were analyzed for multiple performance metrics, including specific fuel consumption (SFC), emissions, exergy destruction, and exergetic efficiency. Calculated by dividing the fuel consumption rate by the engine's output power, providing insight into fuel efficiency. CO, CO_2, HC, O_2, and NO_x levels were analyzed to determine the environmental impact of each fuel blend. The reduction or increase in emissions was used to evaluate the effectiveness of the octanol and hexanol mixtures in lowering pollutants. Energy, Exergetic destruction, Thermoeconomic, exergoeconomic analysis and efficiency were calculated to assess how effectively each fuel blend converted energy into useful work. Detailed information about calculation is given in the third section. Exergetic efficiency was compared to pure gasoline (G100) to determine the benefits or drawbacks of octanol and hexanol additions. The results were statistically analyzed to ensure repeatability and consistency, and all calculations accounted for uncertainties. This comprehensive approach allowed for a detailed assesment of the two-stroke UAV engine's performance across different fuel types and operating conditions.

Table 3
Properties of octanol, hexanol and gasoline fuels.

Property	Gasoline [40]	Octanol [41]	Hexanol [41]
Viscosity (cSt at 40 °C)	0.61	5.8	4.64
Density (kg/m^3 at 15 °C)	747.6	827	821.8
Lower Heating Value (LHV) (MJ/kg)	41.4	37.53	36.4
Octane Number (RON)	95	106	73
Oxygen Content (% by weight)	0	12.29	15.7

Table 4
Measurement device sensitivity and calculated uncertainties.

Parameter	Sensitivity	Tolerance	Remarks
Shaft Speed (rpm)	1 rpm	±0.5 %	Includes resolution and repeatability uncertainty.
Thrust (kg)	±0.01 kg	±0.1 %	Resolution and calibration-related uncertainty.
Fuel Flow Time (s).	±0.1 s	±0.1 s	Chronometer precision
Surface Temperature (°C)	±2°C	–	Thermal camera precision
Exhaust Gas Temperature (°C)	±0.1 °C	–	K-type thermocouple precision
CO (%vol)	0.001 % vol	±0.005 % vol	Combines device sensitivity and tolerance.
CO_2 (%vol)	0.01 %vol	±0.2 %vol	Combines device sensitivity and tolerance.
HC (ppm vol)	1 ppm vol	±12 ppm	Combines device sensitivity and tolerance.
O_2 (%vol)-	0.01 %vol	±0.4 %vol	Combines device sensitivity and tolerance.

3. Thermodynamic analysis

3.1. Energy analysis

In the UAV two-stroke engine, the energy input consists of the energies from air ($\dot{N}_{air}$) and fuel($\dot{N}_{fuel}$), while the energy output includes shaft work ($\dot{SFT}_{work}$), exhaust energy ($\dot{N}_{exh}$), and lost energy($\dot{N}_{lost}$), all measured in kW. If we assume that the temperature of the intake air (T_{air}) entering the system stays constant, the $\dot{N}_{fuel}$ can be expressed as the total of $\dot{SFT}_{work}$, $\dot{N}_{exh}$, and $\dot{N}_{lost}$ energies, as indicated in Eq. (1) [42].

$$\dot{N}_{fuel} = \dot{SFT}_{work} + \dot{N}_{exh} + \dot{N}_{lost} \tag{1}$$

Eq. (2) [43] can be utilized to calculate the fuel energy of a UAV two stroke engine operating at rpm range of 3250 and 6250. In this formula, m denotes the mass flow rate(MFR) of the fuel in kg/s, and N signifies the Q_{fuel} of the fuel in kJ/kg.

$$\dot{N}_{fuel} = \dot{m}_{fuel} Q_{fuel} \tag{2}$$

The torque of the two stroke UAV engine(T_{UAV}, Nm) can be calculated using Eq. (3), which considers the thrust force (F_T, N) measured during the tests (49, 98, 147, 196, and 245 N) and the thrust arm length(L) of 3.65x10^{-2} m. To determine the $\dot{SFT}_{work}$ of the UAV two-stroke engine, both the engine speed(n) and the calculated T_{UAV} value are utilized, as expressed in Eq. (4). [44].

$$T_{UAV} = F_T L \tag{3}$$

$$\dot{SFT}_{work} = 2\pi \frac{n.T_{UAV}}{60} \tag{4}$$

Eq. (5) allows for the calculation of the $\dot{N}_{exh}$ emitted from the UAV two-stroke engine system. In this equation, m_i indicates the MFR of the burn gas in kg/s, and h_i denotes the specific enthalpy of the combustion gas at that same state in kJ/kg [45].

$$\dot{N}_{exh} = \sum_{i=1}^{n} m_i h_i = m_{CO} h_{CO} + m_{CO2} h_{CO2} + \cdots \tag{5}$$

When the $\dot{SFT}_{work}$ of a UAV two stroke engine is divided by the $\dot{N}_{fuel}$ consumed, the thermal efficiency = energy efficiency (η_I) is derived, as shown in Eq. (6) [46].

$$\eta_I = \frac{\dot{SFT}_{work}}{\dot{N}_{fuel}} \tag{6}$$

3.2. Exergy analysis

Exergy illustrates the concept of energy degradation and serves as a measure of the effective work that can be extracted from usable energy. Eq. (7) presents the exergy balance in line with the second law of thermodynamics, where $\dot{X}_{in}$ denotes the incoming exergy flows and $\dot{X}_{out}$ denotes the outgoing exergy flows, and $\dot{X}_D$ represents the exergy that has been destroyed [47].

$$\dot{X}_{in} = \dot{X}_{out} + \dot{X}_D \tag{7}$$

As seen in Eq. (8), $\dot{X}_{in}$ consists of fuel exergy($\dot{X}_F$), while the total $\dot{X}_{out}$ includes $S\dot{F}T_{work}$, exhaust exergy loss($\dot{X}_x$), heat transfer loss($\dot{X}_h$), and exergy destruction($\dot{X}_d$). The $\dot{X}_F$ is obtained by multiplying the fuel's lower heating value (Q_{fuel}), MFR($\dot{m}$), and the chemical exergy coefficient (ε_{fuel}). To calculate the fuel exergy, Eq. (9) can be used [42]. The fuel's chemical exergy coefficient was determined by Kotas and can be calculated using Eq. (10) [48]. In this calculation, the compound mass ratios of the fuel (k = h/c, m = o/c, and n = s/c) are incorporated.

$$\dot{X}_F = S\dot{F}T_{work} + \dot{X}_x + \dot{X}_h + \dot{X}_d \tag{8}$$

$$\dot{X}_F = \dot{m}_{fuel} Q_{fuel} \varepsilon_{fuel} \tag{9}$$

$$\varepsilon_{fuel} = 1.0401 + 0.1728k + 0.0432m + 0.2169n(1 - 2.0628k) \tag{10}$$

To calculate the exergy of the exhaust gases emitted after combustion from the UAV two-stroke engine, Eq. (11) can be used [49]. In this equation, $\dot{m}_i$ represents the MFR of the burned gases (such as CO, CO_2, etc.) at state i. $\varepsilon_{tm,i}$ denotes the thermochemical exergy, while

$\varepsilon_{ch,i}$ symbolizes the specific chemical exergy. The sum of both parameters and the product of the MFR of the burned gas at state i gives the $\dot{X}_x$. $\varepsilon_{tm,i}$ can be calculated using Eq. (12), whereas $\varepsilon_{ch,i}$ can be determined with Eq. (13) [50]. In Eq. (12), the symbols $\bar{h}$, $\bar{s}$, and T_0 represent enthalpy, entropy, and dead state temperature, respectively. In Eq. (13), $\overline{R}$ is included as the universal gas constant in the calculations. Additionally, in Eq. (13), $\varepsilon_{exh,i}$ and $\varepsilon_{env,i}$ denote the molar ratios of the specified gas component and the i component in the reference environment, respectively[51].

$$\dot{X}_x = \sum_{i=1}^{n} \dot{m}_i [\varepsilon_{tm,i} + \varepsilon_{ch,i}] \tag{11}$$

$$\varepsilon_{tm,i} = \sum_{i=1}^{n} \left[\left(\bar{h}_i - \bar{h}_{i,0} \right) - T_0 \left(\bar{s}_i - \bar{s}_{i,0} \right) \right] \tag{12}$$

$$\varepsilon_{ch,i} = \overline{R} T_0 \sum\nolimits_{i=1}^{n} \left[ln \frac{\varepsilon_{env,i}}{\varepsilon_{exh,i}} \right] \tag{13}$$

The heat transfer loss from the surfaces of the UAV two-stroke engine can be calculated using Eq. (14), which incorporates the dead state temperature(T_0), the surface temperature(T_s), and lost energy of the engine [52,53].

$$\dot{X}_h = \sum \dot{N}_{lost} \left[1 - \frac{T_0}{T_s} \right] \tag{14}$$

In order to obtain exergy efficiency, it is sufficient to proportion the shaft work to the total fuel exergy as seen in Eq. (15) [54].

$$\eta_{II} = \frac{S\dot{F}T_{work}}{\dot{X}_F} \tag{15}$$

3.3. Thermoeconomic and exergoeconomic analysis

Thermoeconomic and exergoeconomic analysis are engineering approaches, and thermoeconomic analysis combines thermodynamic and economic analysis, while exergoeconomic analysis combines exergy and economic analyses. This study uses the EXCEM method (exergy-cost-energy-mass) proposed by Rosen and Dinçer[55] for thermoeconomic and exergoeconomic analyses. The aim here is to combine the engine's energy efficiency and economic performance using thermoeconomic and exergoeconomic methods and provide an assessment. The termoeconomic factor (C_{en}) for the UAV two-stroke engine is obtained by utilizing energy loss($\dot{N}_{lost}$) and capital cost(C_{cost}). Eq. (16) can be employed to determine the termoeconomic factor. When calculating the cost of capital, factors such as the technological infrastructure, design, production, assembly, and operational costs of the system to be established are taken into account, and the resulting numerical values may vary from country to country. Therefore, in this study, the cost incurred during energy and exergy losses (in energy and exergy efficiency transformations) is determined by assuming a fixed value for the cost of capital. In the study, the cost of capital is assumed to be $100,000 to simplify the analysis calculations and ensure the clarity of the resulting analysis outcomes[47,55].

$$C_{en} = \frac{\dot{N}_{lost}}{C_{cost}} \tag{16}$$

The exergoeconomic analysis of the UAV two-stroke engine can be conducted using Eq. (17), which involves dividing the heat transfer loss and exergy destruction by the capital cost [55].

$$C_{ex} = \frac{\dot{X}_h}{C_{cost}} + \frac{\dot{X}_d}{C_{cost}} \tag{17}$$

4. Experimental results

4.1. Engine performance

Fig. 2 demonstrates the variation in SFC for different fractions of fuel blends (gasoline, octanol, and hexanol) according to shaft speed. At lower engine speeds, higher SFC is observed, while an increase in engine speed leads to a decrease in SFC values. In two-stroke engines, having the exhaust valve and intake port open simultaneously at low rpm adversely affects the fresh charge in the cylinder. Additionally, at lower engine speeds, the duration during which both the exhaust and intake ports remain open is longer. This situation prevents some fresh charge from entering the combustion chamber and leads to poor combustion. As

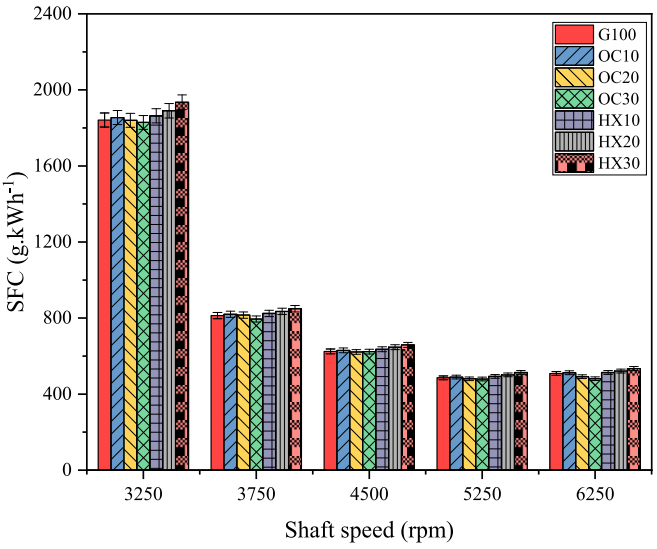

Fig. 2. The variation of SFC versus shaft speed for different fractions of fuel blends (gasoline, octanol, and hexanol).

engine speed increases, the duration for which the intake and exhaust ports are simultaneously open decreases. Furthermore, with increased turbulence at higher speeds, the exhaust gases in the cylinder can be expelled more efficiently from the combustion chamber. All these phenomena affect combustion performance, resulting in changes in SFC values. Additionally, an increase in shaft speed enhances turbulence kinetic energy and vortex formation within the cylinder [56]. Turbulence and vortex formation promote a homogeneous air/fuel mixture inside the cylinder and facilitate the rapid propagation of the flame front. This contributes to an improvement in combustion efficiency, leading to a lower SFC. Across all speeds, the lowest SFC value is attained with OC30 fuel, followed by OC20 and G100 fuels. The highest SFC values occur at 3250 1/min with HX30 fuel. Octanol has a higher octane number than gasoline and hexanol, which allows for a lower knocking tendency and higher flame temperatures during combustion. Additionally, it contributes to the acceleration of unburned HC and CO reactions under high combustion temperature conditions, thereby enhancing combustion efficiency. Furthermore, the O_2 content in octanol improves the homogeneity of the in-cylinder mixture and supports the development of a more efficient combustion phase. All these factors contribute to the reduction of SFC. Moreover, the longer chain structure and higher LHV of octanol than hexanol contribute to lower SFC formation. In a study conducted by Vallinayagam et al.[57], which is consistent with the results of the present study, it was reported that the addition of octane enhancers to gasoline reduces the knocking tendency, improves the combustion phase, and consequently decreases SFC. Generally, when evaluating the average increase/decrease rates within the range of 3250 to 6250 shaft speeds, the SFC values of OC10 increase by 1 % compared to G100, while the SFC values of OC20 and OC30 decrease by 1 % and 2 %, respectively. In the hexanol blends, there are generally increases in SFC values. Compared to G100 fuel, the SFC values for HX10, HX20, and HX30 increase by an average of 1.4 %, 2.9 %, and 5.2 %, respectively. The lower octane number and LHV of hexanol compared to other fuels reduce these values in their mixture. This results in lower combustion temperatures and efficiency, leading to an increase in SFC.

Fig. 3 demonstrates the variation in exhaust gas temperature (EGT) for different fractions of fuel blends (gasoline, octanol, and hexanol) according to shaft speed. With the increase in shaft speed from 3250 rpm to 6250 rpm, the EGT values have shown an upward trend. That is why the improved combustion process that develops with the increase in shaft speed. As seen in the SFC graph (Fig. 1), the fuel consumption of the two-stroke gasoline engine decreases with increasing engine speed. This can be explained by better mixture formation in the cylinder, high turbulence, and the resulting advanced combustion process. Additionally, although the combustion duration shortens with an increase in shaft speed, the combustion phase shifts toward the expansion stroke. This contributes to the rise in EGT. The higher EGT observed with hexanol fuel can be attributed to delayed evaporation, ignition, and an extended combustion duration. Another study by Nora et al. [58] identified increased EGT with increasing speed in two-stroke engines. In their research, it was reported that EGT increases with higher speeds for both oxygenated fuel (ethanol) and gasoline. This study obtained the lowest EGT value with G100 fuel at 3250 1/min, followed by OC10 and HX10 fuels. The highest EGT values were achieved with HX30 fuel at 6250 1/min. Generally, when evaluating the average increase/decrease rates within the range of 3250 to 6250 shaft speeds, the EGT values of OC10, OC20, OC30, HX10, HX20, and HX30 fuels increase by 1 %, 4 %, 5.3 %, 2 %, 3.5 %, and 12.7 %, respectively, compared to G100 fuel.

Lambda is defined as the ratio of the actual air/fuel mixture to the theoretical air/fuel mixture. A lambda value close to 1 indicates that combustion occurs under stoichiometric conditions, whereas a value greater than > 1 shows that combustion takes place under lean conditions [58]. As lean combustion conditions increase, the combustion temperatures decrease due to reduced energy density, which in turn lowers the flame speed. These conditions slow down combustion reactions, leading to lower efficiency and higher fuel consumption. However, the physicochemical structure of oxygenated fuels (such as having a high octane number) can enhance flame speed and combustion temperatures, as observed in OC30 fuel. Fig. 4 demonstrates the variation in lambda for different fractions of fuel blends (gasoline, octanol, and hexanol) according to shaft speed. It is observed that the lambda values are quite close to each other in the shaft speed range of 3250 to 5250 rpm, while at 6250 rpm, the lambda values show a slight increase. Also, the higher lambda values compared to G100 are due to the O_2 content in the octanol and hexanol fuels. Overall, in the shaft speed range of 2350 to 6250 rpm, the lambda values of OC10, OC20, OC30, HX10, HX20, and HX30 fuels increase by an average of 0.4 %, 1 %, 1.1 %, 1.3 %, 2.3 %, and 3.5 %, respectively, compared to G100. Nora and Zhao [59], in their study, stated that an increase in engine speed up to a certain point reduces the air/fuel ratio, resulting in combustion occurring under a richer mixture, which lowers the lambda value. However, the same study reported that further increases in engine speed, along with lower intake air pressure conditions, result in a faster heat release

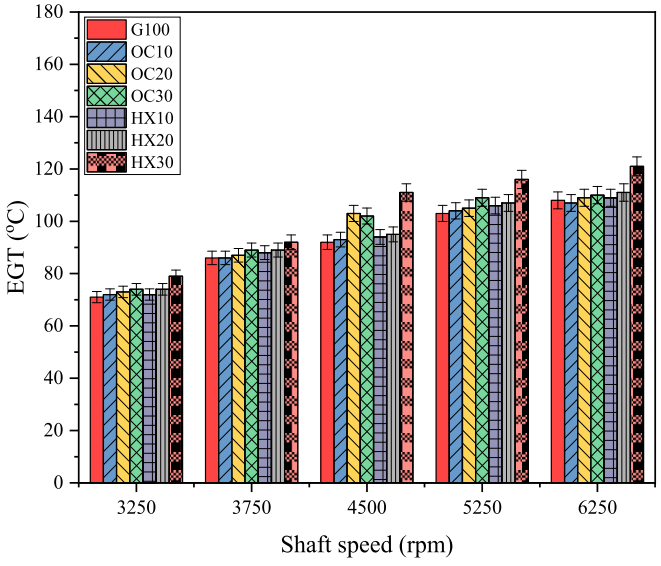

Fig. 3. The variation of EGT versus shaft speed for different fractions of fuel blends (gasoline, octanol, and hexanol).

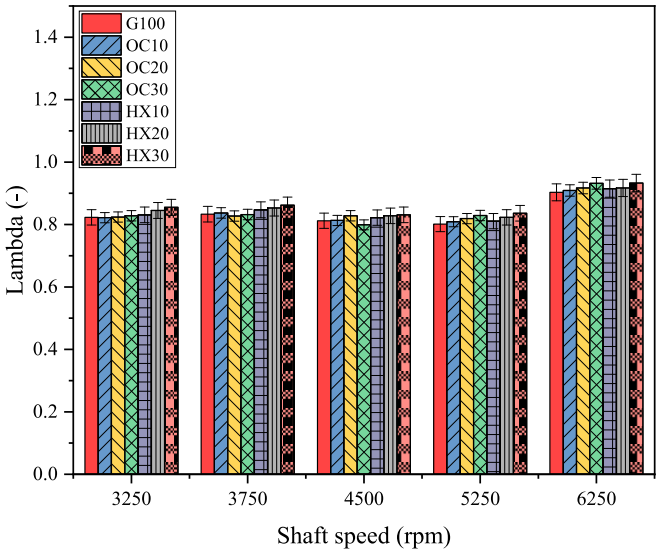

Fig. 4. The variation of lambda versus shaft speed for different fractions of fuel blends (gasoline, octanol, and hexanol).

rate and leaner combustion, leading to an increase in the lambda value compared to lower speeds.

4.2. Engine out-emissions

Fig. 5(a) demonstrates the variation in HC emissions for different fractions of fuel blends (gasoline, octanol, and hexanol) according to shaft speed. In a two-stroke UAV engine, higher HC emissions are observed at low shaft speeds, while HC emissions show a decreasing trend with increasing shaft speed. However, at 6250 rpm, this decreasing trend in HC emissions reverses, remaining lower than the levels observed at low rpms. HC emissions are incomplete combustion products of a rich mixture and can occur due to issues such as leakage from the exhaust valve, surface wear of the valve seat, valve overlap, or fuel properties that lead to low combustion efficiency. The highest HC emissions in an UAV engine are achieved with HX30 fuel at 3250 1/min, while the lowest HC emissions are observed with OC30 fuel at 5250 1/min. Overall, in the rpm range of 3250 to 6250, the HC emissions of OC10, OC20, and OC30 fuels decrease by an average of 3 %, 5 %, and 6 %, respectively, compared to G100, while the HC emissions of HX10, HX20, and HX30 fuels increase by an average of 3 %, 5.5 %, and 7.5 %, respectively. With the increase in shaft speed, a reduction in the fresh charge ratio within the cylinder may lead to an expected rise in HC emissions. However, the increased turbulence and vortex formation at high speeds promote the formation of a homogeneous mixture within the cylinder. Additionally, the higher combustion temperatures and EGT associated with increased speed ensure the continuation of HC and CO emission reactions. Furthermore, blending an O_2-enriched fuel with gasoline can enhance combustion efficiency by increasing the O_2 content in the combustion zone, thereby supporting ongoing chemical reactions. These combined processes result in a decrease in HC and CO emissions as the engine speed increases, a finding consistent with the results of Ghazikhani et al.[25], who reported that adding oxygenated fuel (ethanol) to a two-stroke gasoline engine under high EGT conditions reduces HC and CO emissions.

Fig. 5(b) demonstrates the variation in CO emissions for varying fractions of fuel blends (gasoline, octanol, and hexanol) according to shaft speed. CO emissions generally arise from low combustion temperatures and oxygen content and are incomplete combustion products of a rich mixture. When the carbon (C) in the fuel does not find enough O_2 in a rich mixture, it cannot convert to CO_2 and completes its oxidation as CO [60]. In two-stroke engines, as the engine speed increases, the duration for which the intake and exhaust ports remain open decreases. This results in reduced cylinder filling and increased retention of residual gases. The temperature of the residual gases rises due to delayed combustion at higher speeds (reflected in increased EGT values). This, in turn, increases the temperature of the charge within the cylinder. CO emissions require the presence of O_2 and high temperatures for the conversion of carbon (C) into CO_2. Therefore, a significant increase in temperatures accelerates the reactions that convert CO into CO_2. Additionally, using alcohols with O_2 content in the fuel can reduce CO formation, as they increase the O_2 concentration in the combustion zone. In

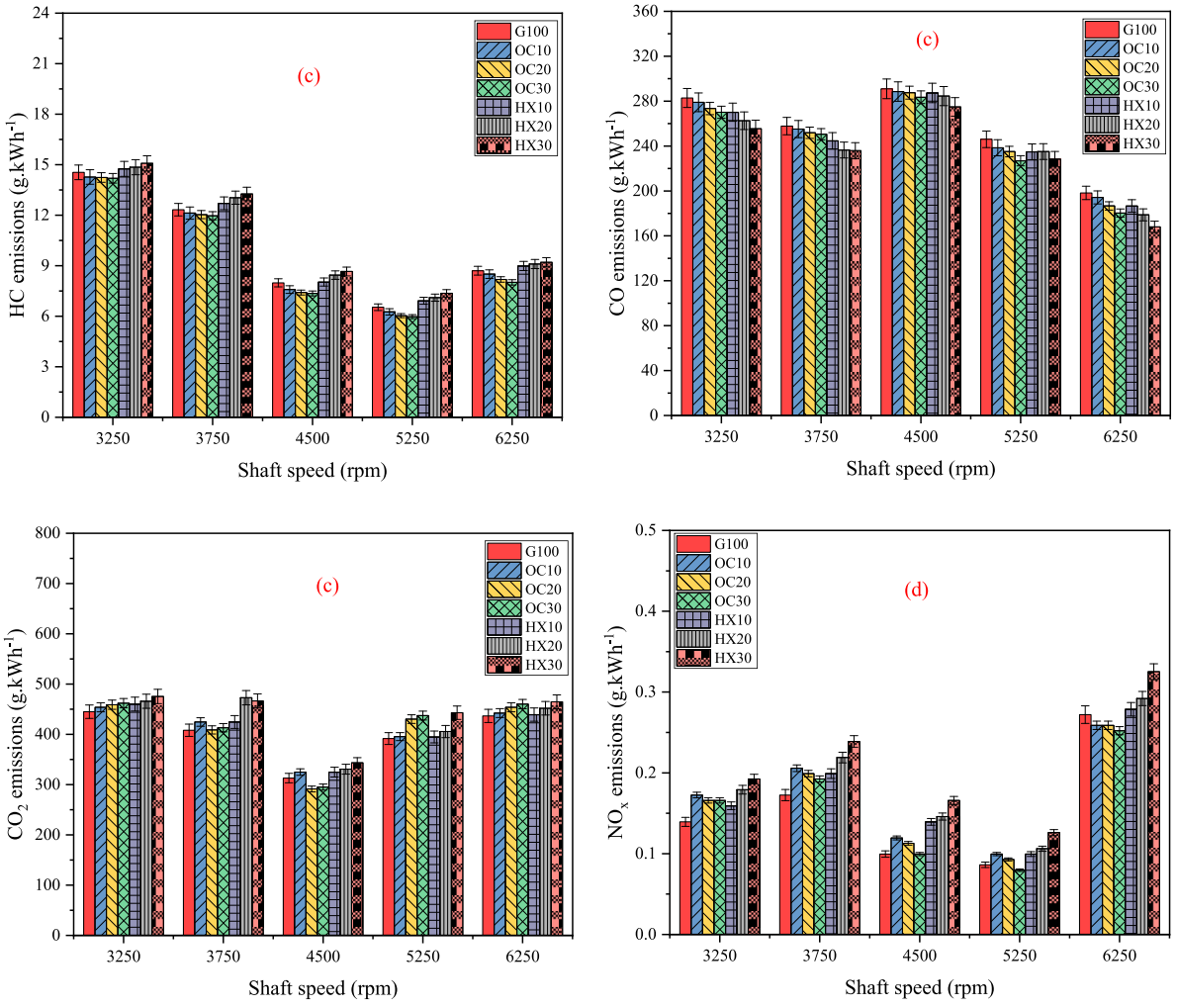

Fig. 5. The variation of (a)HC, (b)CO, (c)CO_2, and (d)NO_x emissions versus shaft speed for different fractions of fuel blends (gasoline, octanol, and hexanol).

the current study, the addition of octanol and hexanol to gasoline reduces CO emissions. In the two-stroke UAV engine, the highest CO emissions at all shaft speeds are achieved with G100, while the lowest CO pollutants are observed with HX30 fuel. Overall, in the rpm range of 3250 to 6250, the CO emissions of OC10, OC20, OC30, HX10, HX20, and HX30 fuels decrease by an average of 1.7 %, 3.4 %, 5.3 %, 4.2 %, 6.4 %, and 9.2 %, respectively, compared to G100.

Fig. 5(c) demonstrates the variation in CO_2 emissions for different fractions of fuel blends (gasoline, octanol, and hexanol) according to shaft speed. CO_2 is a product of complete combustion, and the C/H ratio of the fuel mixture tends to increase with the total amount of fuel consumed or under efficient combustion conditions [61]. In the two-stroke UAV engine, the highest CO_2 emissions are generally obtained with fuels containing octanol and hexanol, primarily due to their high O_2 content. The lowest CO_2 emission level is achieved at 4500 shaft speed across all rpm conditions. Conversely, the highest CO emissions occur at the same rpm. This indicates that at 4500 shaft speed, CO emissions do not convert to CO_2 due to insufficient O_2 in the combustion zone, where excessively rich or lean mixture regions prevent homogeneous mixing. Consequently, while CO_2 emissions are minimized, a trade-off relationship leads to maximum CO emissions. In the two-stroke UAV engine, the highest CO_2 emissions at all shaft speeds are attained with HX30, while the lowest CO_2 emissions are attained with G100. Overall, in the rpm range of 3250 to 6250, the CO_2 emissions of OC10, OC20, OC30, HX10, HX20, and HX30 fuels increase by an average of 2.4 %, 2 %, 3.3 %, 2.5 %, 6.7 %, and 10.1 %, respectively, compared to G100.

Fig. 5(d) demonstrates the variation in NO_x emissions for different fractions of fuel blends (gasoline, octanol, and hexanol) according to shaft speed. According to the Zeldovich mechanism, the main sources of NO_x emissions are high O_2 levels and combustion temperatures [62]. In the current two-stroke UAV engine, NO_x emissions are relatively low compared to other emissions. The primary reason for this is that combustion occurs under rich mixture conditions, as seen in the lambda graph above. Generally, at all speeds, the highest NO_x emissions are attained with HX30 fuel, followed closely by HX20 fuel. It can be stated that the high O_2 concentration in hexanol fuel supports NO_x formation. Additionally, as indicated by the EGT measurements, the highest gas temperatures are associated with hexanol-blended fuels. This can be explained by both the high O_2 content and the elevated gas temperatures contributing to the formation of NO_x emissions. Overall, the lowest NO_x emissions for the two-stroke UAV engine are obtained at 5250 1/min, while the highest NO_x emissions are recorded at 6250 1/min. In the rpm range of 3250 to 6250, the NO_x emissions of OC10, OC20, OC30, HX10, HX20, and HX30 fuels increase by an average of 14.7 %, 10.1 %, 3.1 %, 17.5 %, 26.5 %, and 42 %, respectively, compared to G100.

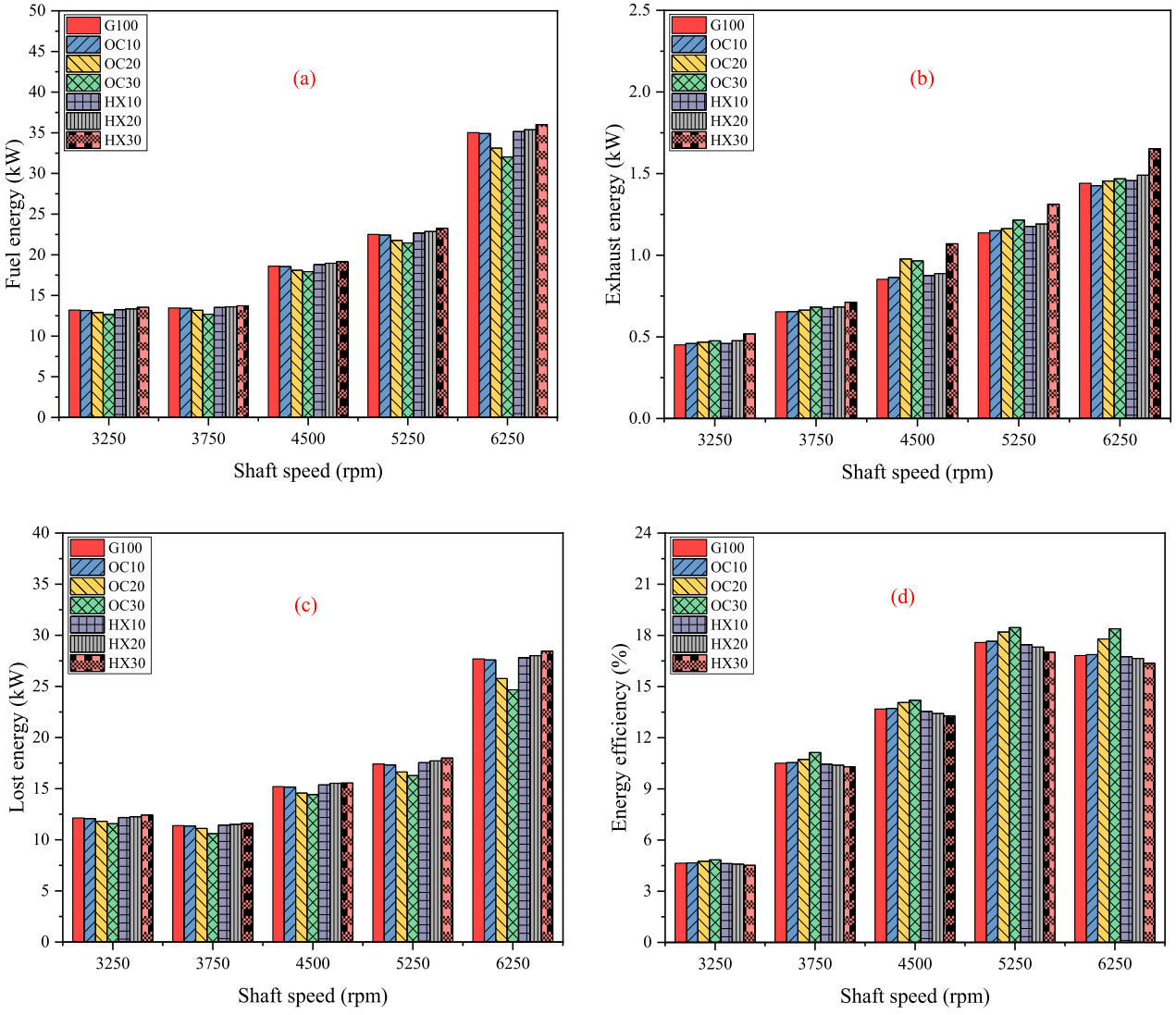

Fig. 6. The variation of (a)fuel energy, (b)exhaust energy, (c)lost energy, and (d)energy efficiency versus shaft speed for different fractions of fuel blends (gasoline, octanol, and hexanol).

Overall, the balance between HC, CO, CO_2, and NO_x emissions depends on the combustion conditions and engine operating parameters. In a rich mixture, incomplete combustion leads to an increase in HC and CO emissions, while in a lean mixture, the rise in combustion temperature causes an increase in NO_x emissions. Engine load, temperature, and oxygen content create a balancing mechanism between these pollutants.

5. Thermodynamic analysis results

5.1. Energy analysis

Fig. 6(a) demonstrates the variation in fuel energy for varying fractions of fuel blends (gasoline, octanol, and hexanol) according to shaft speed. At all shaft speeds, adding octanol to gasoline reduces fuel energy, while adding hexanol to gasoline results in the opposite effect. For example, between shaft speeds of 3250 and 6250, the maximum decrease in fuel energy of OC10 compared to G100 is 0.5 %, while the maximum decrease for OC30 is 8.5 % compared to G100. The average decrease in fuel energy of OC10, OC20, and OC30 compared to G100 is 0.3 %, 3.2 %, and 5.3 %, respectively. In the case of hexanol fuel, it is observed that the increase in the blending ratio with gasoline results in an increase in fuel energy. Between shaft speeds of 3250 and 6250, the maximum increase in fuel energy of HX10 compared to G100 is 1 %, while the maximum increase for HX30 is 3.4 % compared to G100. The average increase in fuel energy of HX10, HX20, and HX30 compared to G100 is 0.6 %, 1.3 %, and 2.8 %, respectively. Overall, it can be concluded that gradually increasing the addition of octanol to gasoline leads to a decrease in fuel energy, while the gradual increase of hexanol results in an increase in fuel energy. The high O_2 content of octanol contributes to the rapid evaporation of the fuel and promotes a more homogeneous distribution of the charge, facilitating faster chemical reactions. Additionally, with its high octane number, octanol provides low knock tendency and high combustion temperatures, which in turn contribute to an increase in combustion efficiency. These factors collectively enable the required power to be achieved with less fuel consumption and, consequently, lower energy demand. The findings obtained in the current article appear to be consistent with the literature. Demirbas and Yesilyurt [63] reported that the addition of 25 % hexanol by volume to gasoline reduced the LHV of the mixture and led to higher fuel consumption due to lower energy content. As a result, they noted that fuel energy increased while energy efficiency decreased.

Fig. 6(b) demonstrates the variation in exhaust energy for different fractions of fuel blends (gasoline, octanol, and hexanol) according to shaft speed. Both octanol and hexanol additions to gasoline contribute to an increase in exhaust energy. The exhaust gas mass flow rate and EGT directly influence exhaust energy. The high EGT values of octanol and hexanol blends increase the enthalpy differences of the gases, which plays a significant role in the rise of exhaust energy. Furthermore, the lower LHV of hexanol than the other two fuels leads to higher SFC, consequently increasing the exhaust mass flow rate. The increase in both parameters is the primary reason for the rise in exhaust energy. Between shaft speeds of 3250 and 6250, the maximum increase in exhaust energy of OC10 compared to G100 is 1.9 %, while the maximum increase for OC30 compared to G100 is 13.3 %. The average increases in exhaust energy for OC10, OC20, and OC30 compared to G100 are 0.7 %, 4.6 %, and 6.4 %, respectively. Regarding hexanol-gasoline mixtures, between shaft speeds of 3250 and 6250, the maximum increase in exhaust energy of HX10 compared to G100 is 3.6 %, while the maximum increase for HX30 compared to G100 is 25.6 %. The average increases in exhaust energy for HX10, HX20, and HX30 compared to G100 are 2.5 %, 4.5 %, and 15.9 %, respectively.

Fig. 6(c) demonstrates the variation in lost energy for different fractions of fuel blends (gasoline, octanol, and hexanol) according to shaft speed. The volumetric increase of octanol in gasoline has a positive impact on lost energy. To illustrate, between shaft speeds of 3250 and 6250, the maximum decrease in lost energy of OC10 compared to G100 is 0.6 %, while the maximum decrease for OC30 is 11 % compared to G100. The average decrease in lost energy of OC10, OC20, and OC30 compared to G100 is 0.4 %, 4.2 %, and 6.8 %, respectively. In the case of hexanol fuel, it is observed that the increase in the blending ratio with gasoline results in an increase in lost energy. Between shaft speeds of 3250 and 6250, the maximum increase in lost energy of HX10 compared to G100 is 1.1 %, while the maximum increase for HX30 is 3.3 % compared to G100. The average increase in lost energy of HX10, HX20, and HX30 compared to G100 is 0.6 %, 1.4 %, and 2.5 %, respectively. Overall, it can be concluded that gradually increasing the addition of octanol to gasoline leads to a decrease in lost energy, while the gradual increase of hexanol results in an increase in lost energy.

Fig. 6(d) demonstrates the variation in energy efficiency for different fractions of fuel blends (gasoline, octanol, and hexanol) according to shaft speed. While octanol contributes to increased energy efficiency, hexanol reduces energy efficiency. For example, between shaft speeds of 3250 and 6250, the maximum increase in energy efficiency of OC10 compared to G100 is 0.5 %, while the maximum increase for OC30 is 9.3 % compared to G100. The average increase in energy efficiency of OC10, OC20, and OC30 compared to G100 is 0.3 %, 3.3 %, and 5.7 %, respectively. In the case of hexanol fuel, it is observed that the increase in the blending ratio with gasoline results in a decrease in energy efficiency. Between shaft speeds of 3250 and 6250, the maximum decrease in energy efficiency of HX10 compared to G100 is 1 %, while the maximum decrease for HX30 is 3.3 % compared to G100. The average decrease in energy efficiency of HX10, HX20, and HX30 compared to G100 is 0.6 %, 1.3 %, and 2.7 %, respectively. In summary, the addition of octanol to gasoline has a positive impact on energy efficiency. The oxygen present in octanol contributes to the formation of a more homogeneous charge, enhancing the development of the flame front. As a result, lower fuel energy and higher thermal efficiency are achieved. Similarly, Ahn and colleagues [64] have reported that increasing the proportion of octanol in the fuel improves the combustion process, leading to an increase in energy efficiency. The higher fuel density and lower heating value of hexanol compared to gasoline cause more fuel consumption. This causes the energy efficiency of hexanol to decrease.

5.2. Exergy analysis

Fig. 7(a) demonstrates the variation in fuel exergy for varying fractions of fuel blends (gasoline, octanol, and hexanol) according to shaft speed. As the shaft speed increases, all test fuels tend to increase their fuel exergies. To illustrate, at a shaft speed of 3250, the fuel exergies of G100, OC10, OC20, OC30, HX10, HX20, and HX30 are 14.2 kW, 14.1 kW, 13.9 kW, 13.6 kW, 14.2 kW, 14.4 kW, and 14.6 kW, respectively. At a shaft speed of 6250, the fuel exergies of G100, OC10, OC20, OC30, HX10, HX20, and HX30 are 37.6 kW, 37.5 kW, 35.6 kW, 34.5 kW, 37.8 kW, 38.1 kW, and 38.7 kW, respectively. More fuel is sent to the combustion zone to meet the increasing engine power with rising shaft speed. This results in an increase in fuel exergy with the rise in speed. The fuel exergy results for the test fuels G100, OC10, OC20, OC30, HX10, HX20, and HX30 are higher than fuel energy due to the chemical exergy coefficient. Compared to G100 fuel, the highest reduction rate in fuel exergy occurs with OC30 fuel at 8.4 % (at 6250 shaft speed), while the highest increase rate occurs with HX30 fuel at 3.6 % (at 5250 shaft speed). In general, compared to G100 fuel, the average reduction rates in fuel exergy for OC10, OC20, and OC30 are 0.3 %, 3.1 %, and 5.1 %, respectively, while the average increase rates for HX10, HX20, and HX30 are 0.7 %, 1.5 %, and 3 %, respectively. Similar to the findings on fuel energy, the use of hexanol is seen to increase fuel exergy. The main reason for this is the high density of the fuel, its slow evaporation, and the reduction of the mixture's lower heating value.

Fig. 7(b) demonstrates the variation in exhaust exergy for different fractions of fuel blends (gasoline, octanol, and hexanol) according to shaft speed. The increase of octanol ratio or hexanol ratio in gasoline

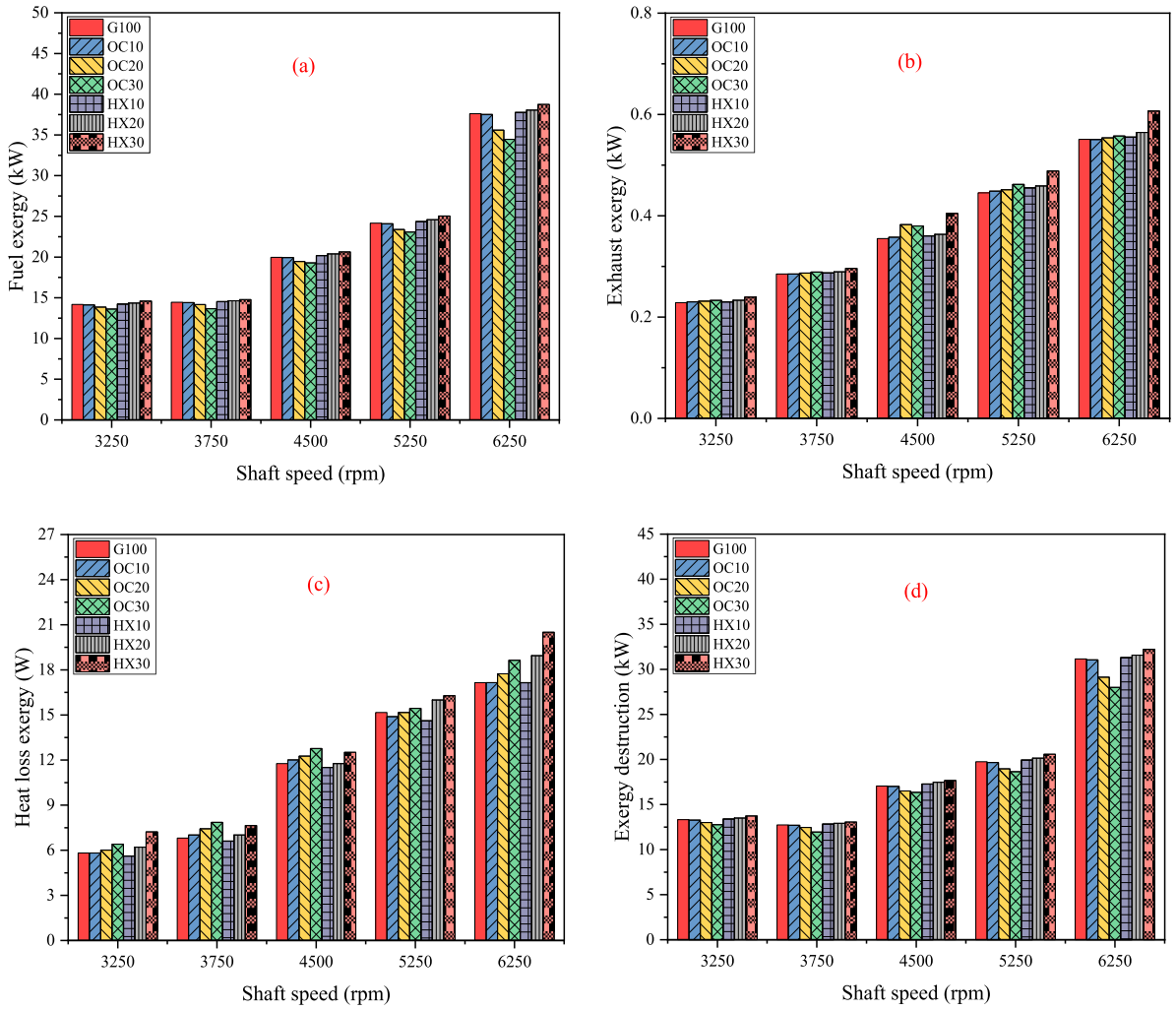

Fig. 7. The variation of (a)fuel exergy, (b)exhaust exergy, (c)heat loss exergy, and (d)energy destruction versus shaft speed for different fractions of fuel blends (gasoline, octanol, and hexanol).

volume raises the loss of exhaust exergy. The highest exhaust exergy value is obtained with HX30 fuel, while the lowest exhaust exergy value is achieved with G100 fuel. For example, between shaft speeds of 3250 and 6250, the maximum increase in exhaust exergy of OC10 compared to G100 is 0.8 %, while the maximum increase for OC30 compared to G100 is 7 %. The average increases in exhaust exergy for OC10, OC20, and OC30 compared to G100 are 0.4 %, 2.3 %, and 3.1 %, respectively. Regarding hexanol-gasoline mixtures, between shaft speeds of 3250 and 6250, the maximum increase in exhaust exergy of HX10 compared to G100 is 2.3 %, while the maximum increase for HX30 compared to G100 is 14 %. The average increases in exhaust exergy for HX10, HX20, and HX30 compared to G100 are 1.2 %, 2.3 %, and 8.5 %, respectively. Due to the high densities and low lower heating values of octanol and hexanol mixtures, greater mass fuel/air consumption occurs. This leads to an increase in exhaust gas flow rate. Additionally, higher fuel exergy results in elevated combustion temperatures, yielding higher EGTs. Consequently, this increases the loss of exhaust exergy [65,66].

Fig. 7(c) demonstrates the variation in heat loss exergy for different fractions of fuel blends (gasoline, octanol, and hexanol) according to shaft speed. Except for the HX10 mixture, the addition of octanol or hexanol to gasoline leads to an increase in heat loss exergy. Overall, the lowest heat loss is achieved with the HX10 mixture, followed by G100 fuel. In the range of shaft speeds from 3250 to 6250, the average increase rates in heat loss exergy for the OC10, OC20, and OC30 mixtures compared to G100 fuel are 0.7 %, 4 %, and 8.9 %, respectively. Within the same speed range, the heat loss exergy of the HX20 and HX30 mixtures increases by an average of 5.1 % and 13.9 % compared to G100 fuel, while the heat loss exergy of the HX10 mixture decreases by an average of 2.4 %. The oxygen content in octanol enhances combustion development. This improved combustion process leads to increased combustion temperatures, resulting in faster heat transfer rates. In contrast, the poor combustion process associated with hexanol usage causes higher fuel consumption and, consequently, longer combustion durations, which also results in elevated combustion temperatures. Thus, a higher heat transfer rate is achieved.

Fig. 7(d) demonstrates the variation in exergy destruction for different fractions of fuel blends (gasoline, octanol, and hexanol) according to shaft speed. As the shaft speed increases, all test fuels show a tendency for their fuel exergies to increase. In all mixtures and G100 fuel, the change in shaft speed from 3250 to 6250 rpm increases exergy destruction. This is owing to the increased friction, non-homogeneous mixtures, high turbulence, and reduced oxygen presence in the combustion zone associated with the rise in speed. These factors increase irreversibility and also exergy destruction. The gradual increase of octanol volume in gasoline progressively reduces exergy destruction, while hexanol yields the opposite effect. For example, in the shaft speed range of 3250 to 6250, the exergy destructions of the OC10, OC20, and OC30 mixtures decrease by an average of 0.3 %, 3.6 %, and 6.1 %, respectively, compared to G100 fuel. Conversely, the exergy destructions of the HX10, HX20, and HX30 mixtures increase by an

average of 0.8 %, 1.7 %, and 3.3 %, respectively, compared to G100 fuel. In conclusion, it can be stated that the fuel with octanol mixtures results in less irreversibility and exergy destruction due to better combustion processes and lower fuel consumption.

Fig. 8 demonstrates the variation in exergy efficiency for different fractions of fuel blends (gasoline, octanol, and hexanol) according to shaft speed. As seen in the figure, the addition of octanol and hexanol to gasoline significantly affects exergy efficiency. While octanol contributes to increased exergy efficiency, hexanol reduces exergy efficiency. The gradual increase of octanol in the gasoline volume gradually increases the exergy efficiency. For example, between shaft speeds of 3250 and 6250, the maximum increase in exergy efficiency of OC10 compared to G100 is 0.4 %, while the maximum increase for OC30 is 9.1 % compared to G100. The average increase in exergy efficiency of OC10, OC20, and OC30 compared to G100 is 0.3 %, 3.2 %, and 5.4 %, respectively. In the case of hexanol fuel, it is observed that the increase in the blending ratio with gasoline results in a decrease in exergy efficiency[30,67]. Between shaft speeds of 3250 and 6250, the maximum decrease in exergy efficiency of HX10 compared to G100 is 1.1 %, while the maximum decrease for HX30 is 3.5 % compared to G100. The average decrease in exergy efficiency of HX10, HX20, and HX30 compared to G100 is 0.7 %, 1.5 %, and 2.9 %, respectively.

5.3. Thermoeconomic and exergoeconomic analysis

The thermoeconomic factor offers insights into the energy loss per unit of capital cost associated with the operation of a single-cylinder, air-cooled, two-stroke UAV engine utilizing various fuel blends at shaft speeds ranging from 3250 to 6250. Fig. 9(a) demonstrates the variation in thermoeconomic factor for different fractions of fuel blends (gasoline, octanol, and hexanol) according to shaft speed. The results show that the lowest thermoeconomic value was obtained in mixtures containing octanol, while the highest thermoeconomic value was obtained in fuels mixed with hexanol. Moreover, the gradual increase in the volume of octanol in gasoline gradually reduces the thermoeconomic factor, while the gradual increase in the volume of hexanol also gradually reduces the thermoeconomic factor. For example, between shaft speeds of 3250 and 6250, the maximum decrease in thermoeconomic factor of OC10 compared to G100 is 0.6 %, while the maximum decrease for OC30 is 10.9 % compared to G100. The average decrease in thermoeconomic factor of OC10, OC20, and OC30 compared to G100 is 0.5 %, 4.2 %, and 6.8 %, respectively. In the case of hexanol fuel, between shaft speeds of 3250 and 6250, the maximum increase in thermoeconomic factor of HX10 compared to G100 is 1.1 %, while the maximum increase for HX30 is 3.3 % compared to G100. The average increase in thermoeconomic factor of HX10, HX20, and HX30 compared to G100 is 0.6 %, 1.4 %, and 2.5 %, respectively. The lower energy loss of the test fuels with octanol results in lower thermoeconomic values, whereas the opposite is true for the test fuels containing hexanol.

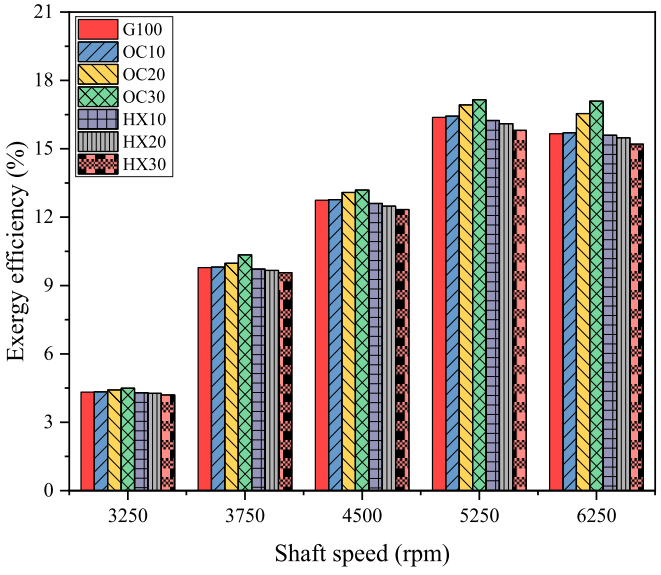

Fig. 8. The variation of exergy efficiency versus shaft speed for different fractions of fuel blends (gasoline, octanol, and hexanol).

The exergoeconomic factor is directly affected by the sum of exergy loss and exergy destruction in the test fuels mixed with gasoline, octanol, and hexanol. Fig. 9(b) demonstrates the variation in exergoeconomic factor for different fractions of fuel blends (gasoline, octanol, and hexanol) according to shaft speed. Similar to the thermoeconomic results, an increase in the octanol ratio in gasoline reduces the exergoeconomic impact, while an increase in the hexanol ratio yields the opposite result. For example, between shaft speeds of 3250 and 6250, the maximum decrease in exergoeconomic factor of OC10 compared to G100 is 0.4 %, while the maximum decrease for OC30 is 10.1 % compared to G100. The average decrease in exergoeconomic factor of OC10, OC20, and OC30 compared to G100 is 0.3 %, 3.6 %, and 6 %, respectively. In the case of hexanol fuel, between shaft speeds of 3250 and 6250, the maximum increase in exergoeconomic factor of HX10 compared to G100 is 1.3 %, while the maximum increase for HX30 is 4.2 % compared to G100. The average increase in exergoeconomic factor of HX10, HX20, and HX30 compared to G100 is 0.8 %, 1.7 %, and 3.3 %, respectively. The higher exergy destruction and exergy loss in hexanol mixtures compared to gasoline and octanol mixtures lead to an increase in the exergoeconomic factor. In contrast, the lower exergy destruction and exergy loss in octanol mixtures compared to both gasoline and hexanol mixtures result in a lower exergoeconomic factor [68,69].

6. Conclusions

In this experimental study, the use of gasoline, gasoline-octanol, and gasoline-hexanol blended fuels in a two-stroke UAV engine has been analyzed and evaluated in terms of performance, emissions, thermodynamics, thermoeconomics, and exergoeconomics. Octanol-gasoline blends are prepared by adding octanol to gasoline in volumetric ratios of 10 % (OC10), 20 % (OC20), and 30 % (OC30). Similarly, hexanol-gasoline blends are created by adding hexanol to gasoline in volumetric ratios of 10 % (HX10), 20 % (HX20), and 30 % (HX30). According to the performance and thermodynamic analysis results, adding 30 % octanol by volume to gasoline generally has a positive effect, while adding 30 % hexanol by volume to gasoline has the opposite effect:

- In the UAV two-stroke engine, the highest SFC value is achieved with HX30 fuel at a shaft speed of 3250 rpm, which represents a 5.1 % increase compared to gasoline. Conversely, the lowest SFC value is obtained with OC30 fuel at a shaft speed of 6250 rpm, showing a 5.3 % decrease compared to gasoline.
- OC30 reduces HC and CO emissions by an average of 6 % and 5.3 %, respectively, while increasing CO_2 and NO_x emissions by an average of 3.3 % and 3.1 %. This is because the high LHV, octane number, and O_2 content of octanol enhance combustion efficiency and improve the stable combustion phase. In contrast, the low octane number and LHV of hexanol increase HC and CO_2 emissions. However, thanks to hexanol's higher O_2 content, CO emissions show the highest average reduction (9.2 %).
- While OC30 reduces fuel exergy (with a max. reduction of 8.4 % at 6250 rpm), HX30 increases fuel exergy by an average of 3 %. The fuel energy results for both fuels also exhibit similar trends. The increase and decrease patterns in SFC significantly influence the analysis results of these two fuels.
- The highest exhaust energy and exergy values in the study are achieved with HX30 fuel. The main reason for this is that HX30 fuel

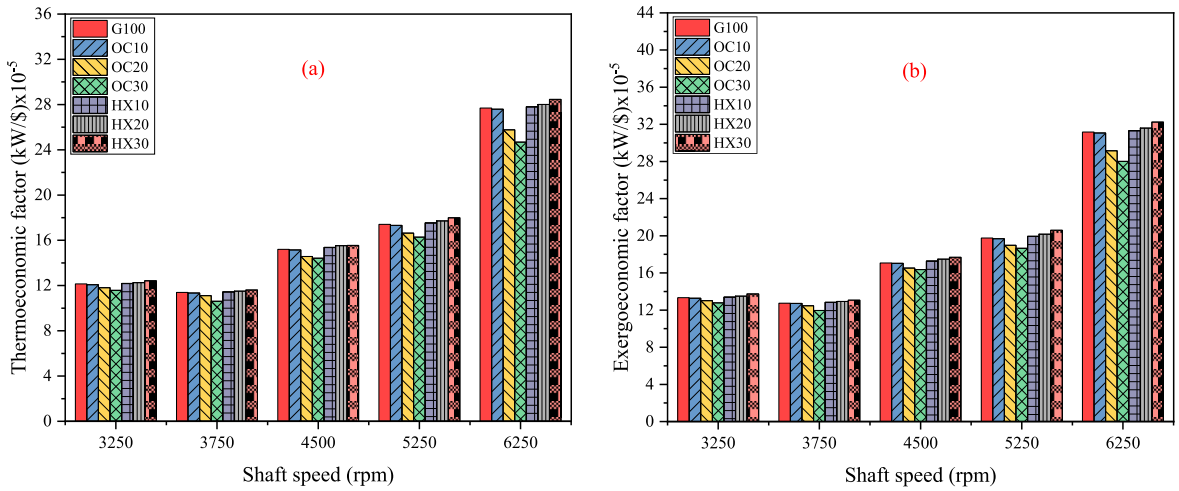

Fig. 9. The variation of (a)thermoeconomic factor, (b)exergoeconomic factor versus shaft speed for different fractions of fuel blends (gasoline, octanol, and hexanol).

increases fuel consumption and exhibits higher EGT values compared to the other fuels.

- The OC30 fuel reduces exergy destruction by a maximum of 10.1 % (at 6250 rpm) and an average of 6.1 %. In contrast, the HX30 fuel increases exergy destruction by a maximum of 4.2 % (at 5250 rpm) and an average of 3.3 %.
- When exergy and thermal efficiencies are examined, the OC30 fuel increases exergy efficiency by a maximum of 9.1 % (at 6250 rpm) and an average of 5.4 %. In contrast, the HX30 fuel reduces exergy efficiency by a maximum of 3.5 % (at 5250 rpm) and an average of 2.9 %. OC30 fuel increases thermal efficiency by an average of 5.7 %.
- Looking at the thermoeconomic results, OC30 reduces the thermoeconomic impact by a maximum of 10.9 % (at 6250 rpm) and an average of 6.8 %. Similarly, the exergoeconomic impact is reduced by a maximum of 10.1 % and an average of 6 %. In contrast, HX30 increases both the thermoeconomic and exergoeconomic impacts.

Strict emission regulations, limited oil reserves, and the fluctuating cost of crude oil make it essential to explore new alternative fuels for internal combustion engines. The use of octanol in this study shows promising results, demonstrating higher energy and exergy performance and lower fuel consumption compared to gasoline and hexanol fuels. However, due to the low demand for alcohol fuels and their limited production, their prices are generally higher than gasoline. Therefore, using alcohol fuels at optimal ratios within gasoline would be more beneficial in terms of both economics and performance. In future studies, the environmental footprint and enviroeconomic impact of the current fuels can be examined to determine their environmental sustainability and raise environmental awareness.

CRediT authorship contribution statement

Salih Özer: Writing – review & editing, Writing – original draft, Validation, Supervision, Resources, Methodology, Investigation, Data curation, Conceptualization. **Erdal Tunçer:** Writing – review & editing, Writing – original draft, Resources, Methodology, Investigation, Data curation, Conceptualization. **Usame Demir:** Writing – review & editing, Writing – original draft, Validation, Methodology, Investigation, Formal analysis, Data curation, Conceptualization. **Halil Erdi Gülcan:** Writing – review & editing, Writing – original draft, Visualization, Validation, Investigation, Formal analysis, Data curation, Conceptualization.

Declaration of competing interest

The authors declare that they have no known competing financial interests or personal relationships that could have appeared to influence the work reported in this paper.

Data availability

Data will be made available on request.

References

[1] Reitz RD, Ogawa H, Payri R, Fansler T, Kokjohn S, Moriyoshi Y, et al. IJER editorial: The future of the internal combustion engine. Int J Engine Res 2020;21:3–10. https://doi.org/10.1177/1468087419877990/ASSET/IMAGES/LARGE/10.1177_1468087419877990-FIG2.JPEG.

[2] Leach F, Kalghatgi G, Stone R, Miles P. The scope for improving the efficiency and environmental impact of internal combustion engines. Transp Eng 2020;1:100005. https://doi.org/10.1016/J.TRENG.2020.100005.

[3] Research AA-IJ of E, 1998 undefined. On the emissions from internal-combustion engines: a review. Wiley Online Libr Abdel-RahmanInternational J Energy Res 1998•Wiley Online Libr n.d.

[4] Winkler SL, Anderson JE, Garza L, Ruona WC, Vogt R, Wallington TJ. Vehicle criteria pollutant (PM, NOx, CO, HCs) emissions: how low should we go? Npj Clim Atmos Sci 2018.1–5.;2018(11):1. https://doi.org/10.1038/s41612-018-0037-5.

[5] Asghar U, Rafiq S, Anwar A, Iqbal T, Ahmed A, Jamil F, et al. Review on the progress in emission control technologies for the abatement of CO2, SOx and NOx from fuel combustion. J Environ Chem Eng 2021;9:106064. https://doi.org/10.1016/J.JECE.2021.106064.

[6] Perera F. Pollution from Fossil-Fuel Combustion is the Leading Environmental Threat to Global Pediatric Health and Equity: Solutions Exist. Int J Environ Res Public Heal 2018, Vol 15, Page 16 2017;15:16. https://doi.org/10.3390/IJERPH15010016.

[7] Brijesh P, Sreedhara S. Exhaust emissions and its control methods in compression ignition engines: A review. Int J Automot Technol 2013;14:195–206. https://doi.org/10.1007/S12239-013-0022-2/METRICS.

[8] Kozina A, Radica G, Nižetić S. Analysis of methods towards reduction of harmful pollutants from diesel engines. J Clean Prod 2020;262:121105. https://doi.org/10.1016/J.JCLEPRO.2020.121105.

[9] Shi C, Chai S, Wang H, Ji C, Ge Y, Di L. An insight into direct water injection applied on the hydrogen-enriched rotary engine. Fuel 2023;339:127352. https://doi.org/10.1016/J.FUEL.2022.127352.

[10] Bao J, Qu P, Wang H, Zhou C, Zhang L, Shi C. Implementation of various bowl designs in an HPDI natural gas engine focused on performance and pollutant emissions. Chemosphere 2022;303:135275. https://doi.org/10.1016/J.CHEMOSPHERE.2022.135275.

[11] Shi C, Cheng T, Yang X, Zhang Z, Duan R, Li X. Implementation of various injection rate shapes in an ammonia/diesel dual-fuel engine with special emphasis on combustion and emissions characteristics. Energy 2024;304:132035. https://doi.org/10.1016/J.ENERGY.2024.132035.

[12] Bao J, Wang H, Wang R, Wang Q, Di L, Shi C. Comparative experimental study on macroscopic spray characteristics of various oxygenated diesel fuels. Energy Sci Eng 2023;11:1579–88. https://doi.org/10.1002/ESE3.1409.

[13] Thangaraja J, Kannan C. Effect of exhaust gas recirculation on advanced diesel combustion and alternate fuels - A review. Appl Energy 2016;180:169–84. https://doi.org/10.1016/J.APENERGY.2016.07.096.

[14] Hountalas DT, Mavropoulos GC, Zannis TC, Schwarz V. Possibilities to Achieve Future Emission Limits for HD DI Diesel Engines Using Internal Measures. SAE Tech Pap 2005. https://doi.org/10.4271/2005-01-0377.

[15] Reji A, Nair PA, Saurav AK, Ismail I, Babu N. Emission Reduction in Four-Stroke S.I Engine Using EGR and Catalytic Converter. Springer Proc Mater 2021;7:109–16. https://doi.org/10.1007/978-981-15-6267-9_13.

[16] Lou D, Kang L, Zhang Y, Fang L, Luo C. Effect of Exhaust Gas Recirculation Combined with Selective Catalytic Reduction on NO xEmission Characteristics and Their Matching Optimization of a Heavy-Duty Diesel Engine. ACS Omega 2022;7:22291–302. https://doi.org/10.1021/ACSOMEGA.2C01123/ASSET/IMAGES/LARGE/AO2C01123_0015.JPEG.

[17] Qiao Y, Lin L, Zhong W, Huang K. Investigation on the Performance Characteristics of 2-Stroke Heavy Fuel Light Aeroengine (2SHFLA) with Different Fuel Injection Systems: Modeling and Comparative Simulation. Energies 2020, Vol 13, Page 5136 2020;13:5136. https://doi.org/10.3390/EN13195136.

[18] Otto A, Agatz N, Campbell J, Golden B, Pesch E. Optimization approaches for civil applications of unmanned aerial vehicles (UAVs) or aerial drones: A survey. Networks 2018;72:411–58. https://doi.org/10.1002/NET.21818.

[19] Mohsan SAH, Khan MA, Noor F, Ullah I, Alsharif MH. Towards the Unmanned Aerial Vehicles (UAVs): A Comprehensive Review. Drones 2022, Vol 6, Page 147 2022;6:147. https://doi.org/10.3390/DRONES6060147.

[20] Cantore G, Mattarelli E, Rinaldini CA. A New Design Concept for 2-Stroke Aircraft Diesel Engines. Energy Procedia 2014;45:739–48. https://doi.org/10.1016/J.EGYPRO.2014.01.079.

[21] Aziz A, Sumeru K, Said M, … MP-IJ of, 2016 undefined. Single-cylinder 125 cc Stepped-piston Engine for Mobility and Portable Power Generation Applications. Acad Aziz, K Sumeru, MFM Said, M Perang, H NasutionInternational J Technol 2016•academiaEdu n.d.

[22] Kenny RG. Developments in Two-Stroke Cycle Engine Exhaust Emissions. Http://DxDoiOrg/101243/PIME_PROC_1992_206_165_02 1992;206:93–106. https://doi.org/10.1243/PIME_PROC_1992_206_165_02.

[23] Martins J, Brito FP. Alternative Fuels for Internal Combustion Engines. Energies 2020, Vol 13, Page 4086 2020;13:4086. https://doi.org/10.3390/EN13164086.

[24] Ghazikhani M, Hatami M, Safari B. The effect of alcoholic fuel additives on exergy parameters and emissions in a two stroke gasoline engine. Arab J Sci Eng 2012;39:2117–25. https://doi.org/10.1007/S13369-013-0738-3/METRICS.

[25] Ghazikhani M, Hatami M, Safari B, Domiri GD. Experimental investigation of exhaust temperature and delivery ratio effect on emissions and performance of a gasoline–ethanol two-stroke engine. Case Stud Therm Eng 2014;2:82–90. https://doi.org/10.1016/J.CSITE.2014.01.001.

[26] Ghazikhani M, Hatami M, Safari B, Ganji DD. Experimental investigation of performance improving and emissions reducing in a two stroke SI engine by using ethanol additives. Propuls Power Res 2013;2:276–83. https://doi.org/10.1016/J.JPPR.2013.10.002.

[27] Pourkhesalian AM, Shamekhi AH, Salimi F. Alternative fuel and gasoline in an SI engine: A comparative study of performance and emissions characteristics. Fuel 2010;89:1056–63. https://doi.org/10.1016/J.FUEL.2009.11.025.

[28] He Z, Zhao W, Liu G, Qian Y, Lu X. Effects of short chain aromatics in gasoline on GDI engine combustion and emissions. Fuel 2021;297:120725. https://doi.org/10.1016/J.FUEL.2021.120725.

[29] Yilmaz N, Atmanli A. Experimental evaluation of a diesel engine running on the blends of diesel and pentanol as a next generation higher alcohol. Fuel 2017;210:75–82. https://doi.org/10.1016/J.FUEL.2017.08.051.

[30] Nour M, Attia AMA, Nada SA. Combustion, performance and emission analysis of diesel engine fuelled by higher alcohols (butanol, octanol and heptanol)/diesel blends. Energy Convers Manag 2019;185:313–29. https://doi.org/10.1016/J.ENCONMAN.2019.01.105.

[31] Masum BM, Masjuki HH, Kalam MA, Palash SM, Wakil MA, Imtenan S. Tailoring the key fuel properties using different alcohols (C2–C6) and their evaluation in gasoline engine. Energy Convers Manag 2014;88:382–90. https://doi.org/10.1016/J.ENCONMAN.2014.08.050.

[32] Fan Y, Duan Y, Han D, Qiao X, Huang Z. Influences of isomeric butanol addition on anti-knock tendency of primary reference fuel and toluene primary reference fuel gasoline surrogates. Https://DoiOrg/101177/1468087419850704 2019;22:39–49. https://doi.org/10.1177/1468087419850704.

[33] Frigo S, Raspolli Galletti AM, Fulignati S, Licursi D, Bertin L, Martinez GA, et al. Synthesis of 1-Hexanol/Hexyl hexanoate Mixtures from Grape Pomace: Insights on Diesel Engine Performances at High Bio-Blendstock Loadings. Energies 2023, Vol 16, Page 6789 2023;16:6789. https://doi.org/10.3390/EN16196789.

[34] Miyamoto N, Ogawa H, Nabi MN. Approaches to extremely low emissions and efficient diesel combustion with oxygenated fuels. Http://DxDoiOrg/101243/1468087001545272 2000;1:71–85. https://doi.org/10.1243/1468087001545272.

[35] Lim CS, Lim JH, Cha JS, Lim JY. Comparative effects of oxygenates-gasoline blended fuels on the exhaust emissions in gasoline-powered vehicles. J Environ Manage 2019;239:103–13. https://doi.org/10.1016/J.JENVMAN.2019.03.039.

[36] Nabi MN, Hustad JE. Influence of oxygenates on fine particle and regulated emissions from a diesel engine. Fuel 2012;93:181–8. https://doi.org/10.1016/J.FUEL.2011.11.019.

[37] Yesilyurt MK, Cakmak A. An extensive investigation of utilization of a C8 type long-chain alcohol as a sustainable next-generation biofuel and diesel fuel blends in a CI engine – The effects of alcohol infusion ratio on the performance, exhaust emissions, and combustion characteristics. Fuel 2021;305:121453. https://doi.org/10.1016/J.FUEL.2021.121453.

[38] Sharbuddin Ali S, Swaminathan MR. Effective utilization of waste cooking oil in a diesel engine equipped with CRDi system using C8 oxygenates as additives for cleaner emission. Fuel 2020;275:118003. https://doi.org/10.1016/J.FUEL.2020.118003.

[39] Yesilyurt MK. A detailed investigation on the performance, combustion, and exhaust emission characteristics of a diesel engine running on the blend of diesel fuel, biodiesel and 1-heptanol (C7 alcohol) as a next-generation higher alcohol. Fuel 2020;275:117893. https://doi.org/10.1016/J.FUEL.2020.117893.

[40] Turkcan A, Ozsezen AN, Canakci M. Effects of second injection timing on combustion characteristics of a two stage direct injection gasoline–alcohol HCCI engine. Fuel 2013;111:30–9. https://doi.org/10.1016/J.FUEL.2013.04.029.

[41] Rajesh Kumar B, Saravanan S, Rana D, Nagendran A. A comparative analysis on combustion and emissions of some next generation higher-alcohol/diesel blends in a direct-injection diesel engine. Energy Convers Manag 2016;119:246–56. https://doi.org/10.1016/J.ENCONMAN.2016.04.053.

[42] Gülcan HE. Effect of methane injection strategy on combustion, exergetic performance, and enviro-economic analyses in a diesel/methane CRDI engine. Appl Therm Eng 2024;243:122654. https://doi.org/10.1016/J.APPLTHERMALENG.2024.122654.

[43] Upadhyay N, Kumar K, Kumar Das R, Kumar GS. A thermodynamic approach to energy, exergy, exergoeconomic, enviroeconomic, and sustainability assessments involving an VCR diesel engine employing third-generation biodiesel with TiO2 NPs and n-heptane. Energy Convers Manag 2024;321:119064. https://doi.org/10.1016/J.ENCONMAN.2024.119064.

[44] Karthickeyan V, Thiyagarajan S, Ashok B, Edwin Geo V, Azad AK. Experimental investigation of pomegranate oil methyl ester in ceramic coated engine at different operating condition in direct injection diesel engine with energy and exergy analysis. Energy Convers Manag 2020;205:112334. https://doi.org/10.1016/J.ENCONMAN.2019.112334.

[45] Karali HI, Caliskan H. Energy, exergy, sustainability, thermoeconomic, exergoeconomic, environmental and environmental-economic effects of novel boron-containing open cell geopolymer filter of a diesel engine on exhaust emissions. Energy 2024;290:130247. https://doi.org/10.1016/J.ENERGY.2024.130247.

[46] Şanlı B, Uludamar E. Effect of hydrogen addition in a diesel engine fuelled with diesel and canola biodiesel fuel: Energetic-exergetic, sustainability analyses. Int J Hydrogen Energy 2024;49:1148–59. https://doi.org/10.1016/J.IJHYDENE.2023.10.128.

[47] Caliskan H, Mori K. Environmental, enviroeconomic and enhanced thermodynamic analyses of a diesel engine with diesel oxidation catalyst (DOC) and diesel particulate filter (DPF) after treatment systems. Energy 2017;128:128–44. https://doi.org/10.1016/J.ENERGY.2017.04.014.

[48] Kotas TJ. The exergy method of thermal plant analysis 2012:328.

[49] Rufino CH, de Lima AJTB, Mattos AP, Allah FUM, Bernal JLL, Ferreira JV, et al. Exergetic analysis of a spark ignition engine fuelled with ethanol. Energy Convers Manag 2019;192:20–9. https://doi.org/10.1016/J.ENCONMAN.2019.04.035.

[50] Moran MJ, Shapiro HN, Boettner DD, Bailey MB (Margaret B. Fundamentals of engineering thermodynamics n.d.:1042.

[51] Caliskan H, Tat ME, Hepbasli A. Performance assessment of an internal combustion engine at varying dead (reference) state temperatures. Appl Therm Eng 2009;29:3431–6. https://doi.org/10.1016/J.APPLTHERMALENG.2009.05.021.

[52] Örs İ, Yelbey S, Gülcan HE, Sayın Kul B, Ciniviz M. Evaluation of detailed combustion, energy and exergy analysis on ethanol-gasoline and methanol-gasoline blends of a spark ignition engine. Fuel 2023;354:129340. https://doi.org/10.1016/J.FUEL.2023.129340.

[53] Doğan B, Özer S, Erol D. Exergy, exergoeconomic, and exergoenvironmental evaluations of the use of diesel/fusel oil blends in compression ignition engines. Sustain Energy Technol Assessments 2022;53:102475. https://doi.org/10.1016/J.SETA.2022.102475.

[54] Canakci M, Hosoz M. Energy and Exergy Analyses of a Diesel Engine Fuelled with Various Biodiesels. Energy Sources, Part B 2006;1:379–94. https://doi.org/10.1080/15567240500400796.

[55] Dincer I, Rosen MA. Energy, environment and sustainable development. Appl Energy 1999;64:427–40. https://doi.org/10.1016/S0306-2619(99)00111-7.

[56] Krishna AS, Mallikarjuna JM, Kumar D. Effect of engine parameters on in-cylinder flows in a two-stroke gasoline direct injection engine. Appl Energy 2016;176:282–94. https://doi.org/10.1016/J.APENERGY.2016.05.067.

[57] Vallinayagam R, Vedharaj S, Roberts WL, Dibble RW, Sarathy SM. Performance and emissions of gasoline blended with terpineol as an octane booster. Renew Energy 2017;101:1087–93. https://doi.org/10.1016/J.RENENE.2016.09.055.

[58] Review B, Cowart JS. Engineering Fundamentals of the Internal Combustion Engine, 2nd Ed. J Eng Gas Turbines Power 2004;126:198–198. https://doi.org/10.1115/1.1669459.

[59] Dalla Nora M, Zhao H. High load performance and combustion analysis of a four-valve direct injection gasoline engine running in the two-stroke cycle. Appl Energy 2015;159:117–31. https://doi.org/10.1016/J.APENERGY.2015.08.122.

[60] Çelebi Y, Cengiz M, Aydın A, Aydın H. A comprehensive review of hexanol and its blends in diesel engines. Energy Convers Manag 2024;321:119004. https://doi.org/10.1016/J.ENCONMAN.2024.119004.

[61] Gültekin N, Gülcan HE, Ciniviz M. The impact of hydrogen injection pressure and timing on exhaust, mechanical vibration, and noise emissions in a CI engine fueled with hydrogen-diesel. Int J Hydrogen Energy 2024;78:871–8. https://doi.org/10.1016/J.IJHYDENE.2024.06.356.

[62] Pulkrabek WW. Engineering fundamentals of the internal combustion engine 2004:478.

[63] Demirbas M, Yesilyurt MK. Investigation of the behaviors of higher alcohols in a spark-ignition engine as an oxygenated fuel additive in energy, exergy, economic, and environmental terms. J Therm Anal Calorim 2023;148:4427–62. https://doi.org/10.1007/S10973-023-11993-W/TABLES/7.

[64] Ahn J, Jang K, Yang J, Kim B, Kwon J. Impact of Using n-Octanol/Diesel Blends on the Performance and Emissions of a Direct-Injection Diesel Engine. Energies 2024, Vol 17, Page 2691 2024;17:2691. https://doi.org/10.3390/EN17112691.

[65] Nemati A, Barzegar R, Khalilarya S. The effects of injected fuel temperature on exergy balance under the various operating loads in a di diesel engine. Int J Exergy 2015;17:35–53. https://doi.org/10.1504/IJEX.2015.069317.
[66] Wang B, Pamminger M, Wallner T. Impact of fuel and engine operating conditions on efficiency of a heavy duty truck engine running compression ignition mode using energy and exergy analysis. Appl Energy 2019;254:113645. https://doi.org/10.1016/J.APENERGY.2019.113645.
[67] Yaman H, Doğan B, Yeşilyurt MK, Erol D. Application of Higher-Order Alcohols (1-Hexanol-C6 and 1-Heptanol-C7) in a Spark-Ignition Engine: Analysis and Assessment. Arab J Sci Eng 2021;46:11937–61. https://doi.org/10.1007/S13369-021-05765-7/FIGURES/11.
[68] Sayin Kul B, Ciniviz M. An evaluation based on energy and exergy analyses in SI engine fueled with waste bread bioethanol-gasoline blends. Fuel 2021;286:119375. https://doi.org/10.1016/J.FUEL.2020.119375.
[69] Liu D, Wang H, Liu H, Zheng Z, Zhang Y, Yao M. Identification of factors affecting exergy destruction and engine efficiency of various classes of fuel. Energy 2020;211:118897. https://doi.org/10.1016/J.ENERGY.2020.118897.